Cell, Vol. 112, 575–587, February 21, 2003, Copyright ©2003 by Cell Press

SAS-4 Is a *C. elegans* Centriolar Protein that Controls Centrosome Size

Matthew Kirkham,[1] Thomas Müller-Reichert,[1] Karen Oegema,[1,2,*] Stephan Grill, and Anthony A. Hyman*
Max Planck Institute of Molecular Cell Biology and Genetics
Pfotenhauerstrasse 108
01307 Dresden
Germany

Summary

Centrosomes consist of a centriole pair surrounded by pericentriolar material (PCM). Previous work suggested that centrioles are required to organize PCM to form a structurally stable organelle. Here, we characterize SAS-4, a centriole component in *Caenorhabditis elegans*. Like tubulin, SAS-4 is incorporated into centrioles during their duplication and remains stably associated thereafter. In the absence of SAS-4, centriole duplication fails. Partial depletion of SAS-4 results in structurally defective centrioles that contain reduced levels of SAS-4 and organize proportionally less PCM. Thus, SAS-4 is a centriole-associated component whose amount dictates centrosome size. These results provide novel insight into the poorly understood role of centrioles as centrosomal organizers.

Introduction

Centrioles consist of a polarized central tube surrounded by a 9-fold symmetric array of singlet, doublet, or triplet microtubules (reviewed in Lange et al., 2000; Marshall, 2001; Preble et al., 2000). Centrioles and related structures, referred to as basal bodies or kinetosomes, are found in most extant eukaryotic lineages, including protists, animals, and plants (fungi and higher plants are notable exceptions). Centrioles/basal bodies likely originated in a common ancestor of most eukaryotic lineages where they were components of larger organelles involved in both nuclear division and cell motility (Cavalier-Smith, 2002; Chapman et al., 2000; Mignot, 1996). For their role in nuclear division, the ancestral centriole-containing organelles are thought to have functioned as microtubule organizing centers (MTOCs). The involvement of centrioles in MTOC function by association with pericentriolar material (PCM) that nucleates and organizes microtubules (Gould and Borisy, 1977) and has been retained in one of the most well-studied centriole-containing structures, the animal centrosome (reviewed in Bornens, 2002; Rieder et al., 2001).

In animal cells, mitotic centrosomes consist of a pair of orthogonally connected centrioles surrounded by an electron dense matrix of PCM. Structural studies in which centrosomes were extracted with chaotropic agents suggest that the PCM contains a matrix of 12–15 nm fibers termed the "centromatrix" (Schnackenberg et al., 1998). The "centromatrix" is tightly associated with the centrioles and directs the recruitment of other centrosomal components including ring-shaped complexes containing γ-tubulin (Moritz et al., 1998; Schnackenberg et al., 1998), a specialized tubulin isoform responsible for the microtubule-nucleating capacity of the PCM (reviewed in Oakley, 2000). Although these studies suggest a mechanism for the targeting of nucleating complexes to centrosomes, the mechanism that links the "centromatrix" to the centrioles remains completely unknown.

In a series of classic experiments, Mazia et al. (1960) demonstrated that a complete centrosome behaves as a pair of "polar organizers". If experimentally divided, each resulting half centrosome organizes a single spindle pole that cannot be divided further. Subsequent electron microscopy by Sluder and Rieder (1985) showed that the number of "polar organizers" correlates with the number of centrioles present. Compelling evidence for the idea that centrioles act as centrosomal organizers was obtained in a recent experiment in which centrioles were dissolved by injection of an antibody directed against a specific tubulin modification. Dissolution of centrioles resulted in dispersion of the PCM, confirming that centrioles organize PCM to form structurally stable centrosomes (Bobinnec et al., 1998).

The cycles of centriole and centrosome duplication are intimately coupled. Centrioles initiate duplication at the onset of S phase in a process that requires Cdk2 (reviewed in Fry et al., 2000; Lange et al., 2000; Sluder and Hinchcliffe, 1999). At this time a generative disc, a precursor of the daughter centriole, forms at right angles to the proximal end of each mother centriole. Daughter centrioles elongate as the cell cycle progresses, reaching full-length by G2/M. During the G2/M transition the centrosomes also mature, accumulating γ-tubulin and other PCM components, and increasing in size and nucleating capacity (reviewed in Palazzo et al., 2000). Thus, one centrosome containing a pair of centrioles is found at each spindle pole during mitosis. The timing of centrosome splitting and the number of centrioles per centrosome at other cell cycle stages varies between cell types (see Discussion). The cycle of centrosome inheritance and duplication has long fascinated cell biologists, but the mechanisms regulating it are for the most part poorly understood.

The *C. elegans* embryo is uniquely suited for studies of centriole function because of the ease with which powerful functional genomic approaches for gene identification can be combined with high-resolution single cell microscopy-based functional assays. In *C. elegans*, RNA-mediated interference (RNAi) can be used to analyze the first mitotic division that occurs in embryos that have been essentially completely depleted of any targeted gene product (Montgomery and Fire, 1998). Combined with the sequenced genome, this has stimu-

*Correspondence: hyman@mpi-cbg.de (A.A.H.); koegema@ucsd.edu (K.O.)
[1]These authors contributed equally to this work.
[2]Present address: CMM-East 3080, 9500 Gilman Drive, La Jolla, California 92093

lated large-scale RNAi-based approaches that will identify many of the important genes required for cell division (Gönczy et al., 2000; Zipperlen et al., 2001). To date, only one *C. elegans* protein required for centriole function, the atypical protein kinase ZYG-1, has been characterized (O'Connell et al., 2001). Depletion of ZYG-1 by RNAi prevents centriole duplication in the embryo, resulting in a very characteristic phenotype in which a normal first division is followed by assembly of monopolar spindles during the second division (O'Connell et al., 2001; Figure 2A). By looking for this phenotype in an RNAi-based functional genomic screen we identified SAS-4, a novel stably associated centriolar protein. Functional analysis of SAS-4 suggests that it is a centriolar component whose amount dictates centrosome size, providing molecular insight into the role of centrioles as centrosomal organizers.

Results

Centrosome Duplication Fails Prior to the Second Mitotic Division in *sas-4(RNAi)* Embryos

During an RNAi-based screen for genes required for cell division we identified a gene, F10E9.8, whose inhibition results in defects in the second embryonic division (Gönczy et al., 2000). To analyze the nature of the division defect, we performed RNAi of F10E9.8 in a strain expressing GFP-α-tubulin and filmed the embryos using spinning disk confocal microscopy. In all F10E9.8(RNAi) embryos filmed (n = 15), microtubule dynamics and spindle assembly were identical to wild-type during the first mitotic division (Figure 1A, top images; see also Supplemental Movies S1 and S2 available at http://www.cell.com/cgi/content/full/112/4/575/DC1). However, as F10E9.8(RNAi) embryos entered their second division, each daughter cell assembled only a single centrosomal microtubule aster. These single asters increased normally in size as the cells entered mitosis, and monopolar spindles were formed (Figure 1A, lower right image, and Supplemental Movies S1 and S2 available at above website).

Assembly of monopolar spindles during the second mitotic division suggested that F10E9.8(RNAi) embryos might be defective in centrosome function. We therefore examined centrosome dynamics using a strain coexpressing GFP-γ-tubulin, a centrosomal marker, and GFP-histone (Figure 1B, see also Supplemental Movies S3 and S4 available at above website). In all F10E9.8 (RNAi) embryos filmed (n = 10), bipolar spindles with wild-type levels of γ-tubulin fluorescence at the spindle poles formed during the first mitotic division (Figure 1B, top images). However, only a single focus of γ-tubulin fluorescence was observed in each daughter cell during the second mitotic division. These single centrosomes accumulated γ-tubulin normally and organized monopolar spindles (Figure 1B, lower right image, and Supplemental Movies S3 and S4 available at above website). Identical results were obtained in fixed F10E9.8(RNAi) embryos stained for three additional centrosomal markers ZYG-9 (Figure 1C; Matthews et al., 1998), AIR-1, and SPD-5 (data not shown; Hamill et al., 2002; Hannak et al., 2001; Schumacher et al., 1998). From these results, we conclude that F10E9.8(RNAi) embryos are defective in centrosome duplication following the first mitotic division.

Database searches revealed a cDNA, yk425b11, corresponding to F10E9.8. PCR with the *trans*-spliced SL2 leader sequence confirmed that this cDNA contains the full-length coding sequence. F10E9.8 codes for a 92 kDa protein with no obvious homologies or motifs except a central coiled-coil domain (Figure 1D). Because inhibition of F10E9.8 function by RNAi results in failure of spindle assembly at the second mitotic division, this gene has been named *sas-4* for *s*pindle *a*ssembly defective.

SAS-4 Is Required for Centriole Duplication

How might the *sas-4(RNAi)* phenotype arise and why does it affect centrosome function during the second but not the first cell division? A previous study of the atypical protein kinase ZYG-1 showed that a normal first division followed by monopolar spindle assembly in the second division is a characteristic phenotype resulting from the inability of RNAi-depleted embryonic cytoplasm to support centriole function (Figure 2A; O'Connell et al., 2001). In *zyg-1(RNAi)* embryos, centriole duplication fails. However, other centriole defects, such as the inability of the daughter centriole to recruit or retain PCM or failure of the daughter centriole to separate from the mother centriole, could also result in a similar defect. To distinguish between these possibilities, we examined wild-type and *sas-4(RNAi)* embryos by correlative differential interference contrast (DIC) microscopy/serial section transmission electron microscopy (TEM; Figures 2B and 2C). Fertilized embryos were filmed using DIC microscopy until metaphase of the first embryonic mitosis. At this stage, embryos were rapidly fixed by laser permeabilization in the presence of glutaraldehyde (Priess and Hirsh, 1986). To count the number of centrioles at each spindle pole, fixed embryos were serially sectioned and analyzed by TEM. Previous work has shown that in wild-type, a pair of centrioles is present at each metaphase spindle pole (Albertson, 1984; O'Connell et al., 2001). We confirmed this in the two wild-type embryos that we sectioned (Figure 2B). Significantly, in the four *sas-4(RNAi)* embryos that we serially sectioned, only one centriole was found at each spindle pole (Figure 2C). From these results, we conclude that SAS-4 is required for centriole duplication in the *C. elegans* embryo.

SAS-4 Localizes to Centrioles Throughout the Cell Cycle

Our phenotypic analysis indicated that SAS-4 is required for centriole duplication, raising the possibility that SAS-4 is a centriolar component. To examine the localization of SAS-4 in vivo, we generated an affinity-purified polyclonal antibody and used it for immunofluorescence of whole worms and fixed embryos. In worms, SAS-4 colocalized with γ-tubulin to centrosomes both in sperm and in the syncytial part of the gonad (Figure 3A). Interestingly, SAS-4 staining in the gonad disappeared as the meiotic nuclei cellularized to form oocytes (Figure 3A), presumably marking the point at which the centrioles are lost during oogenesis. At fertilization, a centriole pair enters the oocyte with the sperm (see Figure 2A). In

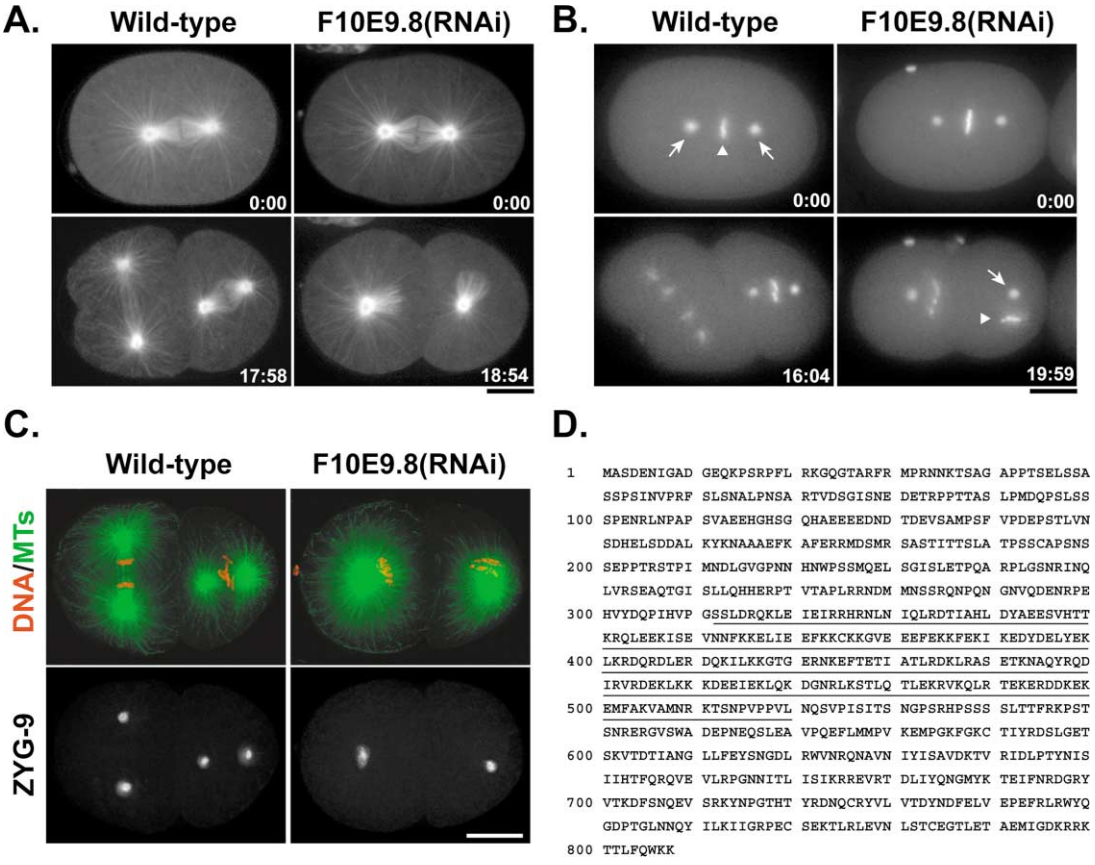

Figure 1. Centrosome Duplication Fails in F10E9.8(RNAi) Embryos

Selected frames from recordings of wild-type and F10E9.8(RNAi) embryos expressing GFP-α-tubulin (A, see also Supplemental Movies S1 and S2 available at http://www.cell.com/cgi/content/full/112/4/575/DC1) or co-expressing GFP-γ-tubulin and GFP-histone (B, see also Supplemental Movies S3 and S4 available at above website). In both strains, F10E9.8(RNAi) embryos assemble normal spindles during the first mitotic division (upper right images in A and B) and monopolar spindles during the second mitotic division (lower right images in A and B). The numbers in the lower right corners of each image show time elapsed from metaphase of the first embryonic mitosis. The arrows in the upper left image of (B) point to the two foci of centrosomal γ-tubulin fluorescence, located on either side of the aligned chromosomes (arrowhead). The arrow and arrowhead in lower right image of (B) point to the single focus of γ-tubulin fluorescence and chromosomes, respectively, in a monopolar spindle.

(C) Two-cell stage wild-type and F10E9.8(RNAi) embryos were fixed and stained for microtubules (MTs) and DNA (green and red in upper images) and the centrosomal protein ZYG-9 (lower images). Only one focus of ZYG-9 staining is seen at the pole of the monopolar spindles in F10E9.8(RNAi) embryos.

(D) F10E9.8 codes for a novel 92 kDa protein with a region predicted to form a coiled coil (underlined). Scale bars are 10 μm.

newly fertilized embryos, SAS-4 is localized to a discrete spot near the sperm-derived pronucleus (Figure 3C, top images). At a slightly later stage, γ-tubulin is recruited to the sperm centrioles forming a focus that colocalizes with SAS-4 (not shown). As the embryo proceeds into mitosis, the amount of γ-tubulin at centrosomes dramatically increases (Hannak et al., 2001; Figure 3C, bottom images). In contrast, the SAS-4 staining remains unchanged as a small dot in the center of the centrosome (Figures 3C and 3E). To confirm the antibody localization, we generated a GFP-SAS-4 expressing strain using microparticle bombardment (Praitis et al., 2001). In living embryos, GFP-SAS-4 fluorescence was observed at a fine focus within centrosomes throughout the cell cycle, similar to the antibody staining (Figures 3B and 3D). From these results, we conclude that SAS-4 localizes to core centrosomal structures, most likely centrioles, throughout the cell cycle.

To examine SAS-4 localization at an ultrastructural level, we performed immunoelectron microscopy on embryos from wild-type hermaphrodites subjected to high-pressure freezing/freeze substitution. In the majority of sections containing centrioles, the secondary antibody conjugated 10 nm colloidal gold particles were observed specifically associated with centriole walls (Figure 3F). In many images, gold particles were detected associated with both mother and daughter centrioles. Cumulatively, the results of the immunofluorescence and immunoelectron microscopy indicate that SAS-4 localizes to centrioles throughout the cell cycle.

SAS-4 Is a Stably Associated Centriole Component that Is Incorporated During Centriole Duplication

To determine if SAS-4 is a stably associated structural component of centrioles, like centriolar tubulin (Kochan-

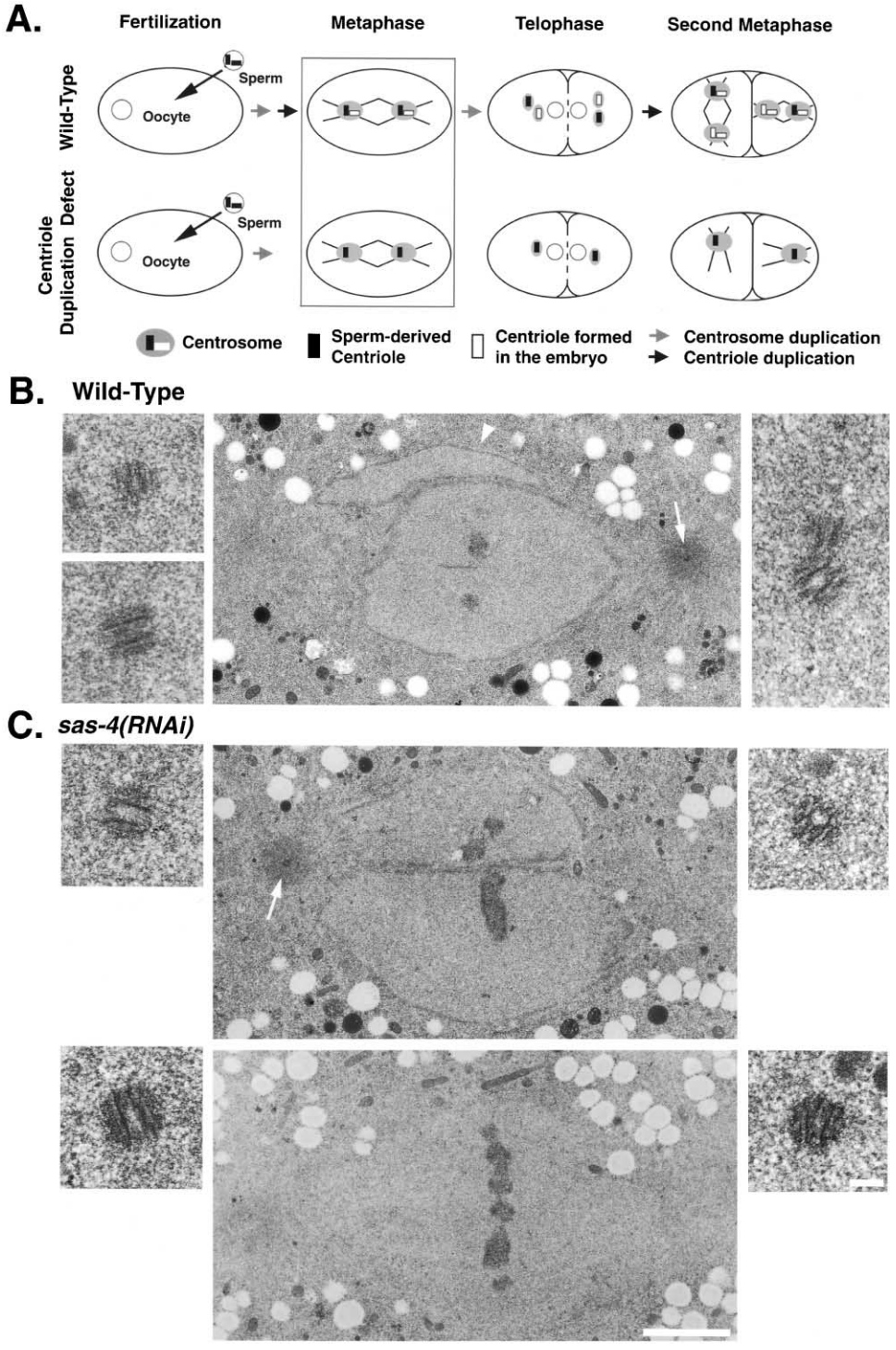

Figure 2. Centriole Duplication Fails in *sas-4(RNAi)* Embryos

(A, top row) Schematic of the centrosome and centriole cycles that follow fertilization in a wild-type *C. elegans* embryo. (Fertilization) During fertilization, the sperm brings a centriole pair into the oocyte, which lacks centrioles (Albertson, 1984; Wolf et al., 1978). (Metaphase) The sperm-derived centriole pair separates and duplicates so that by metaphase of the first mitotic division both spindle poles have a centrosome containing a pair of centrioles (Albertson, 1984; O'Connell et al., 2001). One of the centrioles in each pair was derived from the sperm (black) and the other was formed in the embryonic cytoplasm (white). (Telophase) The centrosomes split (gray arrow) during telophase so that each newly formed daughter cell inherits two centrosomes each containing a single centriole. (Second Metaphase) These centrioles subsequently duplicate (black arrow), so that by metaphase of the second embryonic division each centrosome again contains a pair of centrioles.

(A, bottom row) Schematic of the centrosome and centriole cycles that follow fertilization in an RNAi-depleted embryo that cannot support centriole duplication. Since sperm formation occurs at a developmental stage prior to injection of the interfering dsRNA, a normal centriole pair still enters the oocyte with the sperm during fertilization. These centrioles separate and organize two centrosomes that form the poles of a normal-looking bipolar spindle. However, each metaphase centrosome has only a single sperm-derived centriole. As a consequence of

ski and Borisy, 1990), or whether it is in a dynamic equilibrium with a cytoplasmic pool, we performed a marked mating experiment in which wild-type N2 males were mated to hermaphrodites expressing GFP-SAS-4 (Figure 4). Since male sperm is utilized preferentially over hermaphrodite sperm, this allowed us to introduce centrioles containing exclusively unlabeled SAS-4 into oocyte cytoplasm containing GFP-SAS-4. Embryos were fixed at various times after fertilization and double-label immunofluorescence was performed with the anti-SAS-4 antibody, which detects both the unlabeled SAS-4 and GFP-SAS-4 (Figure 4, total SAS-4), and with an anti-GFP antibody, which selectively detects the GFP-SAS-4 derived from the oocyte cytoplasm (Figure 4, GFP-SAS-4).

In recently fertilized embryos, in which the oocyte pronucleus was still undergoing meiosis, SAS-4 was present as a spot associated with the sperm pronucleus (Figure 4A, total SAS-4). No GFP-SAS-4 was detected, suggesting that SAS-4 associated with the sperm-derived centrioles does not exchange with the cytoplasmic pool (Figure 4A, GFP-SAS-4). By prophase of the first mitotic division, GFP-SAS-4 was detected in the centers of both centrosomes (Figure 4B). The appearance of GFP-SAS-4 coincided with the timing of centriole duplication, presumably reflecting the incorporation of GFP-SAS-4 into daughter centrioles synthesized in the embryo cytoplasm. At metaphase, GFP-SAS-4 continued to be present as a single focus in the center of each centrosome (Figure 4C).

Centrosomes split during telophase, resulting in two centrosomes each of which contains one centriole (see schematic in Figure 4D). This stage is particularly informative because it makes it possible to assay the SAS-4 associated with each centriole independently. Significantly, while both centrosomes contain SAS-4, only one of the centrosomes, most likely the one containing the daughter centriole synthesized in the embryo cytoplasm, contains GFP-SAS-4 (Figure 4D). By prophase of the second mitosis, the centrioles have duplicated again. Both centrosomes now contain at least one centriole that was synthesized in the oocyte cytoplasm and GFP-SAS-4 is detected in the center of both centrosomes (Figure 4E). Interestingly, although the intensity of total SAS-4 staining was equivalent between the two centrosomes in each prophase cell of two-cell embryos, the GFP-SAS-4 staining was asymmetric (Figure 4E). This asymmetry is consistent with one centrosome containing two centrioles formed in the embryo, and the other centrosome containing one unlabeled centriole inherited from the sperm and one centriole formed in the embryo (see schematic to the right of Figure 4). Thus, SAS-4 is a stably associated centriolar component that, like centriolar tubulin, is incorporated during their duplication.

Partial Depletion of SAS-4 Results in Assembly of Centrosomes That Have Less Than Wild-Type Amounts of PCM

Depletion of either ZYG-1 or SAS-4 leads to failure of centriole duplication. To analyze the relationship between the *zyg-1(RNAi)* and *sas-4(RNAi)* phenotypes, we first performed partial RNAi of *sas-4* by varying the time between injection of dsRNA into hermaphrodites and analysis of newly fertilized embryos. Surprisingly, we found that partial *sas-4(RNAi)* led to intermediate phenotypes not previously observed in *zyg-1(RNAi)* embryos. Following partial RNAi of *sas-4*, asymmetric spindles were observed at the two-cell stage in approximately half of the analyzed embryos (Figure 5A; n = 30 embryos; see also Supplemental Movies S5–S7 available at http://www.cell.com/cgi/content/full/112/4/575/DC1). In these spindles, one centrosome had wild-type levels of γ-tubulin whereas the second centrosome had significantly less γ-tubulin and was located closer to the chromosomes. By varying the time of dissection after dsRNA injection, we obtained a continuous range of asymmetric spindles all of which had one normal-looking centrosome and a second centrosome with γ-tubulin levels that varied between normal and barely detectable. These observations suggest that SAS-4 levels dictate the amount of PCM at centrosomes.

To quantitatively compare partial RNAi of *zyg-1* and *sas-4*, we injected hermaphrodites with dsRNA directed against either gene and dissected them after incubation at 16°C for 18, 24, and 28 hr. As a control, we also dissected hermaphrodites injected with *sas-4* RNA that were incubated for 36 hr at 20°C, the conditions used above for stringent RNAi of *sas-4* (Figures 1 and 2). Centrosomes in fixed mitotic two-cell stage embryos were analyzed by staining for γ-tubulin (Figure 5B) and ZYG-9 (not shown). The asymmetry of the centrosome pair in each cell was assessed and classified as either wild-type, asymmetric or, if only one centrosome was present, mono-centrosomal. This analysis revealed that asymmetric spindles are never observed in *zyg-1(RNAi)* embryos. Rather, a threshold level of ZYG-1 is required for centriole duplication to occur (Figure 5C). In contrast, varying SAS-4 levels result in centrosomes of intermediate size (Figures 5B and 5C), suggesting that SAS-4 levels control the amount of PCM at centrosomes.

the failure of centriole duplication, centrosomes fail to split during telophase. Thus, each daughter cell inherits only one centrosome and monopolar spindles form during the second mitotic division.

(B and C) Embryos at the boxed stage in (A) were examined using correlative DIC imaging and serial section TEM. The central images show a single section to give a low-magnification perspective of the analyzed embryo. In wild-type (B), two centrioles were observed at each spindle pole. In the example shown, both centrioles of the right spindle pole were present in the same section (arrow; B, right image); for the left spindle pole, the two centrioles were found in different sections (B, left images).

(C) Two examples of *sas-4(RNAi)* embryos are shown. Only one centriole was found at each spindle pole in all serial sections (shown to the left and right of central images). Note that the nuclear envelopes surrounding the two pronuclei do not completely break down till later in mitosis (the edge of one pronucleus is indicated by an arrowhead in B) and that centrioles in *C. elegans* consist of 9-fold symmetric array of singlet microtubules (Wolf et al., 1978). Scale bars for central overview images are 2.5 μm; scale bars for higher magnification images are 100 nm.

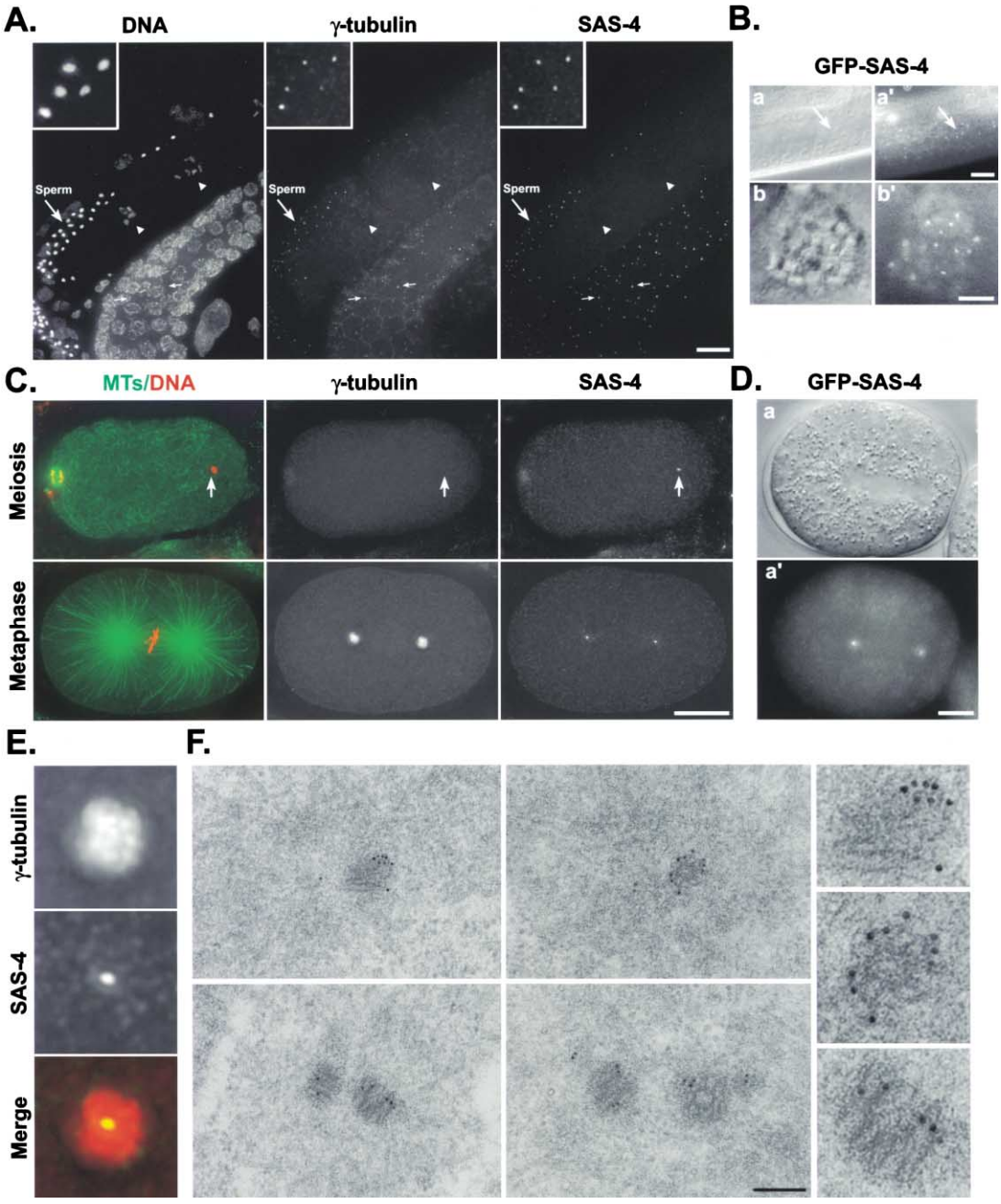

Figure 3. SAS-4 Localizes to Centrioles Throughout the Cell Cycle

(A) Wild-type hermaphrodites were fixed and stained for DNA, γ-tubulin, and SAS-4. SAS-4 colocalized with γ-tubulin to centrosomes in sperm (arrow on left side of all images and insets) and to centrosomes associated with nuclei in meiotic prophase in the gonad arm (small arrows), but disappeared in oocytes (arrowheads). Insets were magnified 3×.

(B) Hermaphrodites expressing GFP-SAS-4 were examined by DIC (a, b) and for GFP fluorescence (a′, b′). As was the case for the SAS-4 antibody staining, single punctate fluorescent foci were found in sperm and associated with meiotic nuclei in the gonad arm. Arrows in (a) and (a′) indicate the location of a cluster of GFP-SAS-4 foci.

(C) Wild-type embryos were fixed and stained to visualize microtubules (MTs) and DNA (green and red in left images), γ-tubulin (middle images), and SAS-4 (right images). In recently fertilized embryos in which the oocyte nucleus was still completing meiosis (top images), SAS-4 was observed in a single punctate focus associated with the sperm pronucleus (arrows). No colocalizing γ-tubulin staining was observed at these early time points. (C) At metaphase, two small foci of SAS-4 staining are seen in the center of the γ-tubulin staining at each spindle pole.

(D) Stills taken from a time-lapse recording of an embryo expressing GFP-SAS-4. Both DIC (a) and GFP fluorescence (a′) are shown. In the DIC image, the mitotic spindle is visible as a region that excludes yolk granules. Punctate foci of GFP-SAS-4 are observed in the center of each spindle pole.

(E) Higher magnification (6.4×) view of the right centrosome in the metaphase image in (C). Scale bars in (A–D) are 10 μm.

(F) Localization of SAS-4 by immunoelectron microscopy. Immunolabeling was found associated with centriole walls. Labeling was detected on both mother and daughter centrioles. Scale bar is 250 nm. Images in the right column show selected centrioles from the images on the left magnified 2.5×.

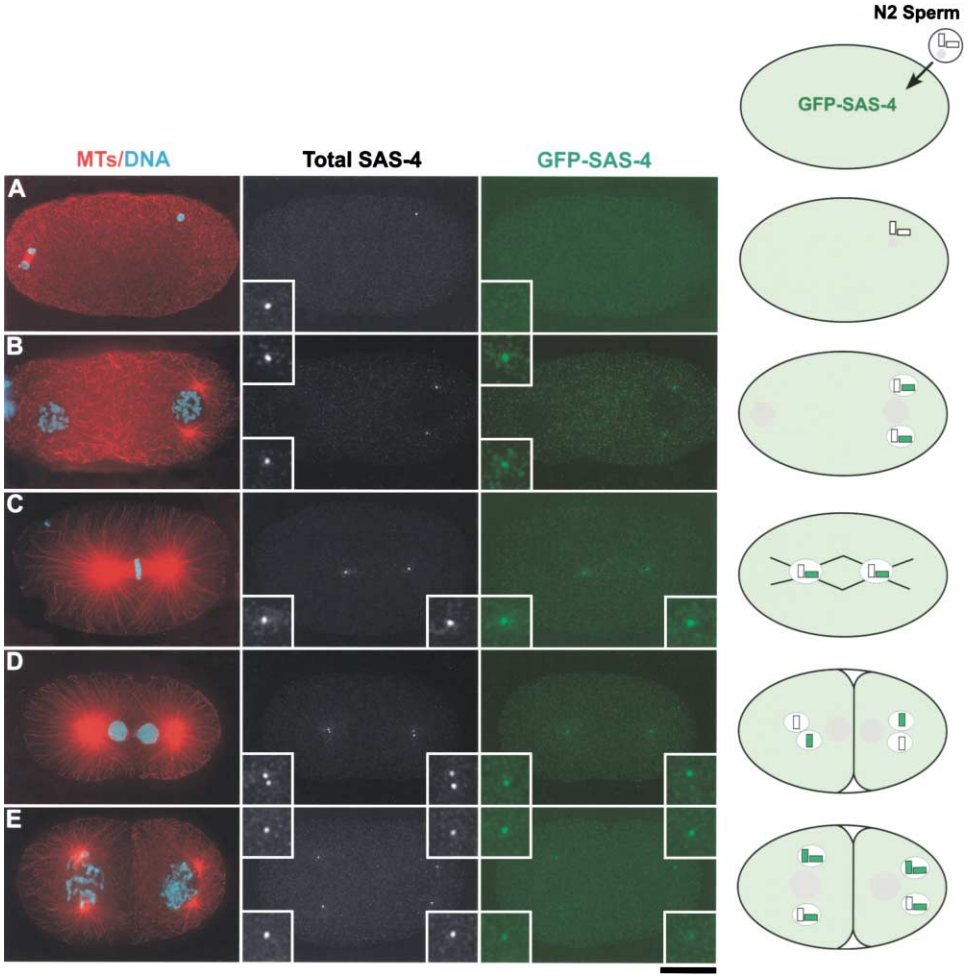

Figure 4. SAS-4 Is Incorporated during Centriole Duplication and Remains Stably Associated Thereafter

Wild-type (N2) males were mated with hermaphrodites expressing GFP-SAS-4. Embryos were fixed at various times after fertilization and stained for microtubules (MTs) and DNA (red and blue in left images) and with antibodies to SAS-4 to detect both the labeled and unlabeled protein (total SAS-4) and to GFP to detect only the GFP-SAS-4 fusion (GFP-SAS-4). Centrosomes are shown in the insets (magnified 3×). A schematic of our interpretation of the results is shown on the right.

(A) In recently fertilized embryos, SAS-4 localizes to the centriole pair associated with the sperm nucleus. There is no staining in the GFP channel.

(B) By prophase of the first mitotic division, GFP-SAS-4 has been incorporated into both centrosomes.

(C) GFP-SAS-4 is also detected in a single focus in the center of each centrosome at metaphase.

(D) When the centrosomes split in telophase, each daughter centrosome inherits one centriole. Both centrosomes have a focus of SAS-4 staining. However, only one of the centrosomes, likely the one containing the daughter centriole synthesized in the embryo, contains GFP-SAS-4.

(E) By prophase of the two-cell stage the centrioles have duplicated again. All of the centrosomes contain at least one centriole that was synthesized in the oocyte cytoplasm and all contain the GFP-SAS-4 fusion protein. Scale bar is 10 μm.

Centriolar SAS-4 Levels Correlate with Centrosome Size

Why does partial RNAi of *sas-4* result in centrosomes of intermediate sizes? A simple hypothesis to explain this observation is that the amount of PCM at a centrosome is proportional to the amount of centriolar SAS-4. To see if this is the case, we performed quantitative immunofluorescence of embryos partially depleted of SAS-4 using directly labeled antibodies against SAS-4 and γ-tubulin. In projections of 3D deconvolved images of mitotic two-cell stage embryos, weaker SAS-4 fluorescence appeared to correlate with weaker γ-tubulin fluorescence at the dim centrosome of the asymmetric centrosome pairs (Figure 6A). To quantify this relationship, we measured total 3D centrosomal SAS-4 and γ-tubulin fluorescence for 14 wild-type and 13 partial *sas-4(RNAi)* centrosome pairs in mitotic two-cell embryos. This analysis confirmed the qualitative observation that the centrosomal fluorescence of both SAS-4 and γ-tubulin at the dim centrosome in *sas-4(RNAi)* embryos was significantly reduced relative to wild-type (Figure 6B, $P < .001$); in contrast, the amount of SAS-4 and γ-tubulin at the bright centrosome of the asymmetric pair in *sas-4(RNAi)* embryos was not significantly different from wild-type (Figure 6B).

To examine the relationship between the amount of

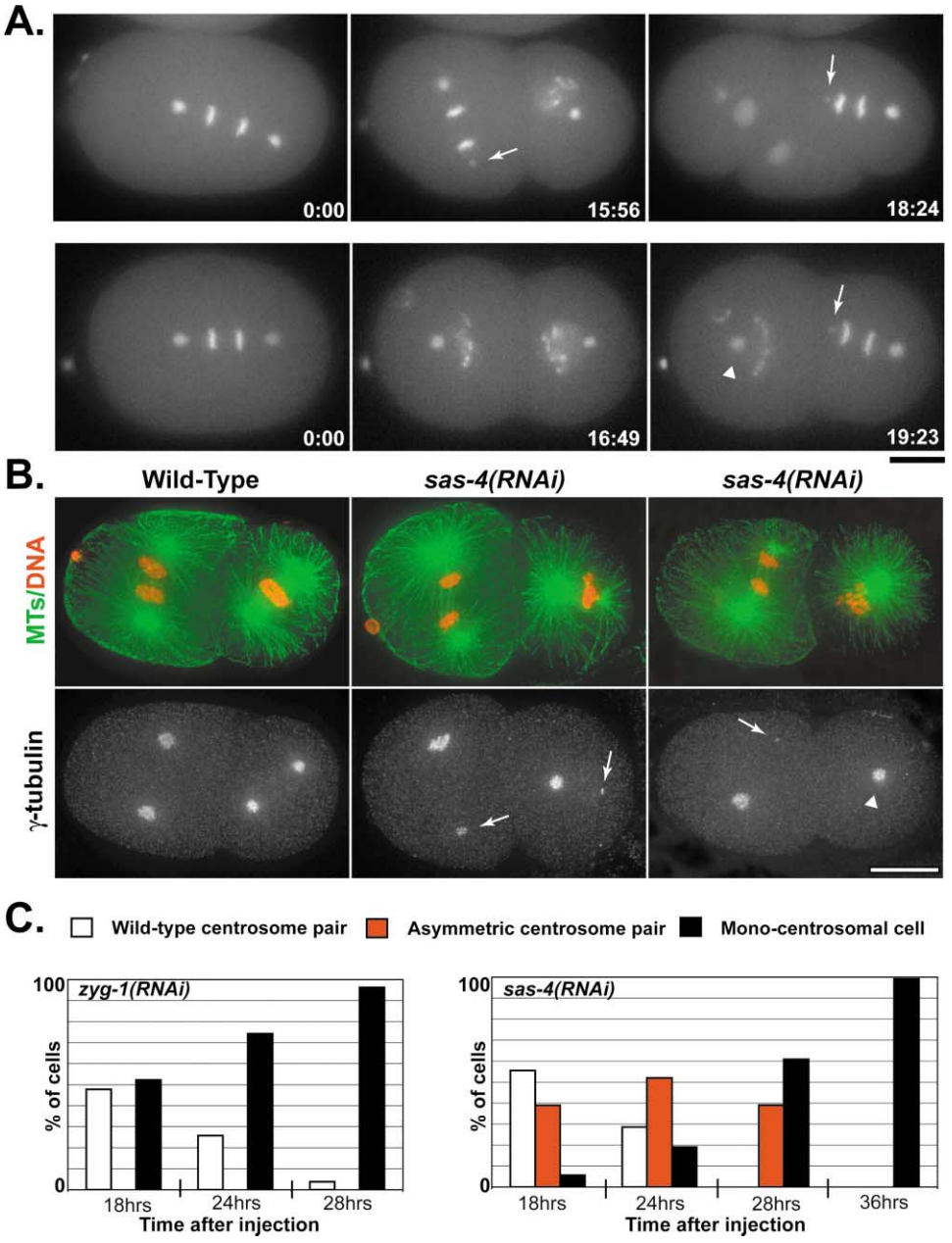

Figure 5. Partial Depletion of SAS-4 Leads to Intermediate Phenotypes Characterized by the Presence of Centrosomes with Less Than Normal Amounts of PCM

(A) Selected frames from two recordings of partial *sas-4(RNAi)* embryos co-expressing GFP-γ-tubulin and GFP-histone (see also Supplemental Movies S5 and S6 available at http://www.cell.com/cgi/content/full/112/4/575/DC1). Numbers in the lower right hand corners are elapsed time. Centrosomes that appear smaller than wild-type (arrows) and a single centrosome in a cell with a monopolar spindle (arrowhead) are indicated.

(B) Partially depleted *sas-4(RNAi)* embryos were fixed and stained to visualize microtubules (MTs) and DNA (green and red in upper images) and γ-tubulin (lower images). A wild-type embryo (left images) and two partially depleted *sas-4(RNAi)* embryos (middle and right images) are shown. Centrosomes that appear smaller than wild-type (arrows) and a single centrosome in a cell with a monopolar spindle (arrowhead) are indicated.

(C) Hermaphrodites were injected with *sas-4* or *zyg-1* dsRNA at the L4 larval stage and allowed to develop for 18, 24, or 28 hr at 16°C. As a positive control, L4 hermaphrodites injected with *sas-4* RNA were incubated for 36 hr at 20°C. Embryos were fixed and stained to visualize microtubules (MTs), DNA, γ-tubulin, and ZYG-9. The fluorescence intensity of the pair of centrosomes in each cell of embryos at the two-cell stage was compared and judged to be wild-type, asymmetric or, if only one centrosome was present, mono-centrosomal. Histograms show the percentage of cells in each phenotypic class for each time point. (Left graph) The number of *zyg-1(RNAi)* cells scored in two-cell stage embryos was 44, 70, and 101 at 18, 24, and 28 hr, respectively. At 18 hr, approximately 50% of cells at the second division in *zyg-1(RNAi)* embryos were wild-type and 50% were mono-centrosomal. After 24 and 28 hr, the percentage of mono-centrosomal cells increased to ~75 and 95%, respectively. At all time points, only wild-type or monopolar spindles were observed in *zyg-1(RNAi)* embryos. (Right graph) The number of *sas-4(RNAi)* cells in two-cell stage embryos scored was 36, 42, 46, and 24 at 18, 24, 28, and 36 hr, respectively. After 18 hr, about 40% of cells in *sas-4(RNAi)* embryos contained spindles with asymmetric centrosomes at their poles. After 24 hr, this percentage increased

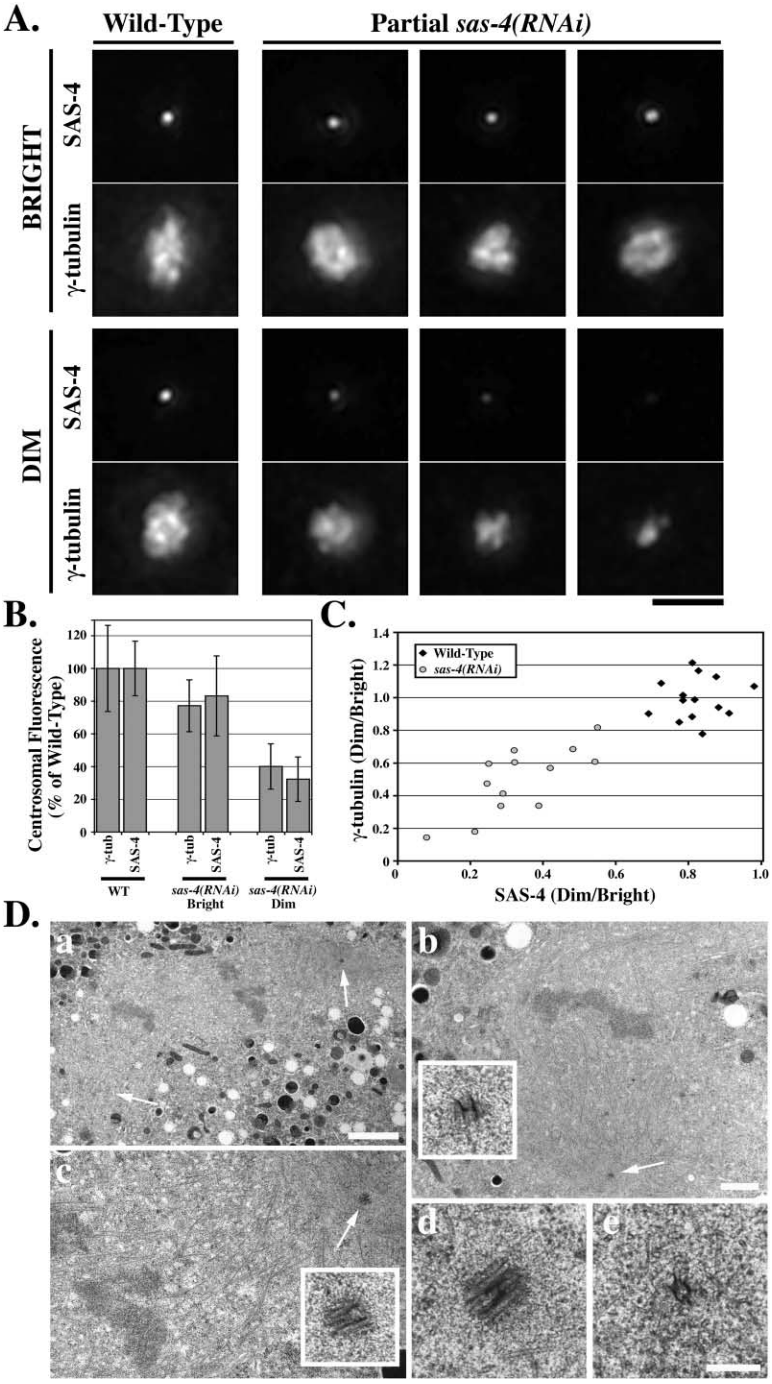

Figure 6. Centrosomal γ-Tubulin Levels Are Proportional to the Amount of Centriolar SAS-4

(A–C) L4 hermaphrodites were injected with *sas-4* RNA and incubated at 20°C for 21–24 hr to produce embryos partially depleted of SAS-4. Embryos were fixed and stained with DAPI to visualize DNA, and with antibodies directly labeled with fluorescent dyes to visualize microtubules, SAS-4, and γ-tubulin. 3D data sets of mitotic embryos at the two-cell stage were collected with an Olympus 100×, 1.35 NA lens using 0.15 μm z steps on a DeltaVision microscope. The centrosomal fluorescence of SAS-4 and γ-tubulin was quantitated in 3D in the deconvolved images (see Experimental Procedures).

(A) Projections of the SAS-4 and γ-tubulin at both centrosomes are shown for one wild-type (left column) and three partial *sas-4(RNAi)* spindles at the two-cell stage. In each case, the centrosome that stained more intensely for SAS-4 (bright) is shown in the top pair of images and the centrosome with weaker SAS-4 staining is shown in the bottom pair of images (dim). As the amount of SAS-4 fluorescence at the dim centrosome decreases, the amount of γ-tubulin fluorescence also decreases.

(B) The average centrosomal γ-tubulin and SAS-4 fluorescence for wild-type and "bright" and "dim" centrosomes in *sas-4(RNAi)* embryos at metaphase is plotted. Error bars are the standard deviation.

(C) For the centrosome pairs in all mitotic wild-type or partial *sas-4(RNAi)* embryos, the ratio of the γ-tubulin fluorescence at the dim centrosome to the fluorescence at the bright centrosome is plotted versus the same ratio for SAS-4.

(D) Centrosomes in partially depleted *sas-4(RNAi)* embryos contain defective centrioles. RNAi was performed by feeding to generate large numbers of worms containing embryos in which SAS-4 was partially depleted. Worms were prepared for TEM by high pressure freezing followed by freeze substitution. (a) Overview showing an anaphase spindle in a two-cell stage embryo. The arrows indicate the approximate positions of the two spindle poles. Scale bar is 2.5 μm. (b) Enlargement of the spindle half on the right side of the image in (a). (c) Enlargement of the spindle half on the left side of the image in (a). The centrioles in (b) and (c) are indicated with arrows. Higher magnification views of both centrioles are shown in the insets. Each pole has only a single centriole and the two centrioles appear to differ in size. Scale bars are 1 μm. (d and e) A similar example from a second embryo. The single centrioles observed at the two poles of a spindle at the two-cell stage are shown, illustrating an apparent difference in the size of the two centrioles. Scale bar is 250 nm.

centriolar SAS-4 and the amount of centrosomal γ-tubulin, we plotted the ratio of total γ-tubulin fluorescence at the dim centrosome to that at the bright centrosome versus the same ratio for SAS-4 for all of the wild-type and partial *sas-4(RNAi)* centrosome pairs. Given that the bright centrosomes in the asymmetric centrosome pairs in *sas-4(RNAi)* embryos are not significantly different from wild-type (Figure 6B), this strategy simplifies the analysis by internally controlling for experimental variations and slight differences in cell cycle state

to just over 50% and cells with monopolar spindles were also observed (~20%). After 28 hr, the number of cells with asymmetric spindles began to decrease (~40%) as the number of cells with monopolar spindles increased to ~60%. After 36 hr at 20°C (the stringent RNAi condition used for *sas-4* in previous experiments), all two-cell embryos had monopolar spindles. Scale bars are 10 μm.

between embryos (Figure 6C). As expected, for centrosome pairs in wild-type embryos the ratio of γ-tubulin (dim/bright) and the ratio of SAS-4 (dim/bright) were always close to one, suggesting that the two centrosomes in each cell contain similar amounts of SAS-4 and similar amounts of γ-tubulin (the ratio of SAS-4 dim/bright is always slightly less than one because we defined the dim centrosome as the one that contains less SAS-4). Interestingly, in the partial *sas-4(RNAi)* embryos, the ratio of γ-tubulin fluorescence at the two asymmetric centrosomes was proportional to the ratio of the SAS-4 fluorescence over a 10-fold range (Figure 6C). This remarkable proportionality strongly suggests that centriolar SAS-4 levels determine centrosome size.

Partial Depletion of SAS-4 Leads to Assembly of Structurally Defective Centrioles

The fact that SAS-4 is a stably associated centriole component required for centriole duplication suggests that the effect of partial SAS-4 depletion on centrosome size could be the result of an alteration in centriole structure. To test this idea, we prepared large numbers of hermaphrodites containing partially depleted embryos by feeding with bacteria expressing dsRNA directed against *sas-4*. Treated hermaphrodites were high pressure frozen, freeze substituted and selected two-cell stage embryos were serially sectioned for TEM analysis. Two of the four serially sectioned embryos that we analyzed had asymmetric centriolar structures at the two spindle poles (Figure 6D). In these embryos, each spindle pole contained a single centriole, suggesting that one round of centriole duplication occurred but the second round, which normally occurs prior to metaphase of the second division, failed. Interestingly, whereas one of the centrioles in each cell had a normal appearance, the second centriole had a smaller, defective, structural appearance (Figure 6Db and 6De). Although 3D EM tomography will be needed to assess the exact nature of the structural alteration in these defective centrioles, these results suggest that reduction of centriolar SAS-4 leads to the formation of structurally compromised daughter centrioles that organize less than wild-type amounts of PCM.

Discussion

SAS-4 Is A Novel *C. elegans* Centriole Component

SAS-4 localizes to core centrosomal structures at all cell cycle stages in the early *C. elegans* embryo. Unlike the PCM components γ-tubulin and ZYG-9, whose amounts at centrosomes increase dramatically as cells enter mitosis (Hannak et al., 2001), centrosomal SAS-4 fluorescence remains constant. Consistent with this, electron microscopy of sections labeled with immunogold localized SAS-4 to the walls of both mother and daughter centrioles. To investigate the timing and dynamic nature of SAS-4 recruitment, we used mating to introduce unlabeled centrioles into oocytes expressing GFP-SAS-4. This experiment is conceptually analogous to a classic experiment in which biotinylated tubulin was microinjected into tissue culture cells to show that the incorporation of tubulin heterodimers into centriolar microtubules is conservative (Kochanski and Borisy, 1990). Our results suggest that SAS-4, like centriolar tubulin, is a stably associated structural component of centrioles that is incorporated during their duplication.

SAS-4 Is Required for Centriole Duplication

Using correlative DIC/TEM microscopy, we have shown that metaphase centrosomes in stringent *sas-4(RNAi)* embryos contain only one instead of the normal two centrioles, demonstrating that SAS-4 is required for centriole duplication. Nevertheless, normal-looking spindles with wild-type levels of γ-tubulin fluorescence at their poles form during the first mitosis in *sas-4(RNAi)* embryos. The lack of a significant difference between centrosomes containing only one centriole and wild-type centrosomes containing two centrioles is consistent with previous work in vertebrate somatic cells demonstrating association of mitotic PCM with only the parent centriole of each pair (reviewed in Vorobjev and Nadezhdina, 1987). In vertebrate somatic cells, daughter centrioles acquire a cloud of fibrillar PCM and the ability to anchor astral microtubules, during prophase of the cell cycle after they are born (Piel et al., 2000; Rieder and Borisy, 1982; Vorobjev and Chentsov, 1982). While our analysis of *sas-4(RNAi)* embryos is consistent with the idea that daughter centrioles do not mature until the cell cycle after their birth, detailed EM analysis of the centriole cycle will be needed to determine the exact timing of daughter centriole maturation in the *C. elegans* embryo.

Our analysis of GFP-SAS-4 in the mating experiment suggests that centriole duplication occurs after centrosome splitting in telophase (Figures 4D and 4E). The centrosome cycle inferred from this result for the *C. elegans* embryo is very similar to the one reported for *Drosophila* embryos (Callaini and Riparbelli, 1990). In both of these embryonic systems, centrosomes contain between 1 and 2 centrioles depending on cell cycle state. The situation is somewhat different in vertebrate somatic cells, where centrosomes contain between 2 and 4 centrioles. In these cells, the mother and daughter centrioles lose their orthogonal orientation in anaphase/telophase (Kuriyama and Borisy, 1981; Rieder and Borisy, 1982; Vorobjev and Chentsov, 1982), but the centrosome does not split because the centrioles are held together until the G2/M transition by a specialized structure that requires the protein C-Nap1 (Fry et al., 1998; Mayor et al., 2000). The similarity of the *C. elegans* and *Drosophila* centrosomal cycles suggests that the centriole-linking structure found in vertebrate somatic cells is not present during embryonic divisions in these systems.

SAS-4 Sheds Light on the Role of Centrioles as Centrosomal Organizers

The amount of SAS-4 at centrioles proportionally dictates the amount of centrosomal PCM. Since stringent RNAi of *sas-4* results in failure of centriole duplication and defective centriolar structures are observed in partial *sas-4(RNAi)* embryos, the effect on centrosome size may be either a direct consequence of depleting SAS-4 or an indirect consequence of perturbing centriole structure. In either case, this work leads to the interesting conclusion that the amount of centrosomal PCM is pro-

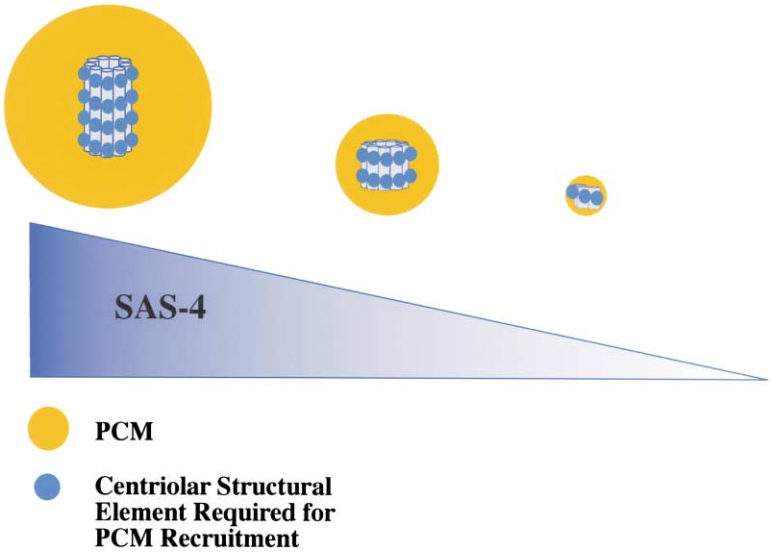

Figure 7. Centriolar SAS-4 Levels Determines Centrosome Size

Decreasing levels of centriolar SAS-4 result in structurally defective daughter centrioles that organize progressively smaller quantities of PCM. In stringent *sas-4(RNAi)* embryos, daughter centrioles fail to form and centrosome duplication fails. These results suggest that an element of centriole structure (blue ovals) is proportionally required to organize PCM (orange). This centriolar element could be SAS-4 itself, or may simply be present at a fixed density on centrioles and hence regulated by SAS-4 levels.

portional to the amount of an element of centriolar structure. In support of a direct role for SAS-4, partial RNAi of other genes involved in centriole function does not lead to a SAS-4-like effect on PCM levels. To date, genetic and functional genomic strategies have identified four *C. elegans* genes including *zyg-1* (O'Connell et al., 2001), *sas-4* (this study), and two novel genes (M.K., K.O. and A.A.H., unpublished data), whose inhibition results in the selective failure of spindle assembly at the second mitotic division characteristic of defects in centriole function. Of these, only SAS-4 results in variably sized centrosomes when partially depleted (Figure 5; M.K., K.O., and A.A.H., unpublished data). Testing the hypothesis that SAS-4 has a direct role in regulating PCM levels will be feasible once the entire genomic complement of genes required for centriole function is identified in *C. elegans*.

How does SAS-4 contribute to centriole-directed centrosome assembly? Our results lead us to conclude that there is an element of centriole structure that is proportionally required to organize PCM. SAS-4 could itself constitute this structural element or be proportionally required for its existence (Figure 7). How does this proposed centriolar element control centrosome size? One possibility is that it directly organizes a defined amount of PCM. Therefore, its centriolar stoichiometry would dictate the extent of PCM recruitment. Alternatively, the centriolar stoichiometry of the proposed element may affect the rate of PCM recruitment or the retention of PCM at centrosomes by activating components for assembly or by affecting their turnover. In addition to control by a centriolar structural element, limiting levels of PCM components also influence centrosome size. An effect of PCM component limitation is expected because centrosomes get smaller when the ratio of cytoplasmic volume to centriole number is reduced during embryonic development.

In summary, our work provides evidence for the existence of a centriolar structural element that proportionally dictates centrosome size. Determining the relationship between SAS-4 and this structural element is an important future goal.

Experimental Procedures

Definition of *sas-4* Coding Sequence

The cDNA, yk425b11, corresponding to F10E9.8 was identified from Yuji Kohara's EST database. Sequencing both strands of this cDNA confirmed the predicted coding sequence but did not reveal an inframe stop codon upstream of the first ATG. To unambiguously assign the start codon, we performed PCR with primers directed against the *trans*-spliced SL2 leader (GGTTTTAACCCAGTTACTC AAG) and an internal region of F10E9.8 (CGCGCGGCGGCCGCC TATTCGGCAGCTGCATTTTTA) using *C. elegans* cDNA as template (gift of Martin Srayko, Max Planck Institute of Molecular Cell Biology and Genetics, Dresden, Germany). AT cloning (Promega) and sequencing of the PCR product confirmed that the ATG present in yk425b11 is the start codon.

RNA-Mediated Interference

For production of dsRNA directed against *sas-4* (TTCCAATGGAT CAACCATCA and TTCCTTTCTCCCGTTCCTTT) and *zyg-1* (TTTTTG TGATCTGCTGGAACA TTTTTGTGATCTGCTGGAACA), the primers in parentheses with tails containing T3 and T7 promoters were used to amplify regions of genomic N2 DNA. PCR products were transcribed and double-stranded RNA prepared as described (Oegema et al., 2001). For all experiments, except the one presented in Figure 6D, dsRNA was injected into L4 hermaphrodites. For stringent RNAi, injected worms were incubated for 28 hr at 25°C (Figures 1A and 1B) or 36 hr at 20°C (Figure 1C and Figure 2). For partial RNAi, injected worms were incubated for 20–26 hr at 25°C (Figure 3A) or for 18–36 hr at 16/20°C, as indicated (Figures 5B and 5C and Figures 6A–6C). To produce large quantities of partially depleted *sas-4 (RNAi)* worms for high pressure freezing (Figure 6D), RNAi was performed by feeding bacteria producing dsRNA to the region of F10E9.8 described above (Timmons et al., 2001).

Generation of GFP-Fusion Expressing Strains and Live Imaging

Strains expressing GFP-α-tubulin and co-expressing GFP-γ-tubulin and GFP-histone H2B were described previously (Oegema et al., 2001). The strain expressing GFP-SAS-4 was constructed by using the primers in parentheses (GCTTCCGCTAGCGCTTCCGATGAA AATATCGGTG, CGCTTCCGCTAGCTCATTTTTTCCACTGGAACAAA GTT) to PCR amplify the genomic F10E9.8 locus. The PCR product was digested with NheI, cloned into the plasmid pAZ132 (gift from Judith Austin, University of Chicago, Chicago, Illinois), and bombarded into *unc-119(ed3)* worms as described (Praitis et al., 2001). Live widefield and spinning disk confocal imaging of embryos expressing GFP fusion proteins was performed as described (Oegema et al., 2001).

Antibody Production

6xHis tagged full-length SAS-4 was prepared by amplifying the cDNA, yk425b11, using the following primers: CGCGCGGGATCCG CTTCCGATGAAAATATCGGTG and CGCGCGCTCGAGTCATTTTT TCCACTGGAACAAAGTT, digesting the product with BamHI/XhoI and cloning into pRSET-A (Invitrogen). Antibodies to the fusion protein were generated in rabbits and affinity purified as described (Oegema et al., 2001). The column for the affinity purification was prepared by coupling a mixture of three GST fusion proteins corresponding to three separate 120 amino acid regions of F10E9.8 to a NHS HiTrap column (Amersham Pharmacia). The following 3 sets of primers: GCGCGCGGATCCATGGCTTCCGATGAAAATATC and GCGCGCCTCGAGTCCACTGTGGCCATGCTCT; GCGCGCGGATCC ATGGCTTCCGATGAAAATATC and GCGCGCCTCGAGTCCACTGT GGCCATGCTCT; GCGCGCGGATCCTCAGCTTCAACAATCACAACA and GCGCGCCTCGAGCTCGGGTCGATTTTCATCTT were used to amplify regions of the cDNA yk425b11. Products were digested with BamHI/XhoI and cloned into pGEX-6P-1 (Amersham Pharmacia). GST fusion proteins were purified and coupled as described (Oegema et al., 2001).

Immunofluorescence, Fixed Imaging, and Quantitation of Centrosomal Fluorescence

Antibodies to γ-tubulin and ZYG-9 were described previously (Hannak et al., 2001). Both antibodies were directly labeled with Cy3 and Cy5 as described (Oegema et al., 2001) and were used at a concentration of 1 μg/ml. DM1α was used at a dilution of 1:1000 to visualize microtubules and polyclonal rabbit anti-GFP (Molecular Probes) was used at 1 μg/ml. In four-color immunofluorescence experiments using anti-SAS-4 and anti-GFP antibodies, embryos were incubated with an excess of goat anti-rabbit Fab fragments (5 μg/ml; Jackson ImmunoResearch Laboratories) to convert the first rabbit antibody to a "goat" antibody before incubation with the second rabbit antibody. For the experiment in Figures 6A–6C, antibodies to SAS-4 were directly labeled with Cy3. Embryos were fixed and processed for immunofluorescence as described (Oegema et al., 2001) and were imaged using a 100×, 1.35 NA objective on an Olympus DeltaVision microscope. All fixed images shown are of 3D widefield data sets that were computationally deconvolved and projected using SoftWorx (Applied Precision). Quantitation of centrosomal fluorescence was performed on deconvolved 3D image stacks as described (Hannak et al., 2002).

Correlative DIC/TEM, High Pressure Freezing/Freeze Substitution, and Immunoelectron Microscopy

For the correlative DIC/TEM in Figure 2, a single wild-type or *sas-4(RNAi)* early embryo was transferred with a mouth pipet to a marked region on an aclar coverslip (Electron Microscopy Sciences) previously glow discharged and coated with 1% poly-L-lysine (Sigma, P1524) in PBS. Water was used to adhere the aclar coverslip to a metal holder before mounting on an inverted microscope (Axiovert 200M, Zeiss). Embryos were imaged through the aclar using DIC until early metaphase. Excess liquid was removed, and the embryo was surrounded with 20 μl of 1× PHEM (60 mM PIPES [pH 6.9], 25 mM HEPES [pH 6.9], 10 mM EGTA, and 2 mM $MgCl_2$) containing 2% glutaraldehyde and 0.4% tannic acid (O'Connell et al., 2001). A pulsed solid-state UV laser (PowerChip, JDS Uniphase) focused with a 63× water immersion objective lens (C-Apochromat, Zeiss) was used for laser permeabilization. About 5 shots were taken at regions where the vitelline membrane touches the eggshell at the very anterior of the embryo and fixation was monitored by live DIC microscopy. Laser and microscope control was based on the CCC software (Alfons Riedinger, Nick Salmon, Ernst H.K. Stelzer, EMBL). After laser permeabilization, embryos were incubated in fixative on ice for at least 30 min, washed 3–4 times in 1× PHEM, and postfixed in 1% osmium tetroxide and 0.5% $K_3Fe(CN)_6$ in 1× PHEM buffer (O'Connell et al., 2001). The samples were dehydrated through a graded acetone series, flat embedded in epon/araldite, and remounted for thin, serial sectioning. Thin sections (70 nm) were cut using a Leica Ultracut UCT microtome. Sections were collected on Formvar-coated copper grids, poststained with 2% uranyl acetate in 70% methanol followed by aqueous lead citrate and viewed in a Philips TECNAI 12 transmission electron microscope operated at 100 kV. For the experiment in Figure 6, partially depleted *sas-4(RNAi)* hermaphrodites prepared by feeding were cryoimmobilized using an HPM 010 high pressure freezer (BAL-TEC). Samples were processed for freeze substitution as described (Rappleye et al., 1999). For immunolabeling experiments, cryoimmobilized wild-type hermaphrodites were freeze substituted at −90°C for 3 days in acetone containing 0.2% glutaraldehyde and 0.1% uranyl acetate. Dehydrated specimens were thin layer embedded in LR White (Lonsdale et al., 2001). Thin sections (50–70 nm) were labeled using anti-SAS-4 diluted in blocking buffer containing 0.8% bovine serum albumin, 0.01% Tween 20, and 0.1% fish scale gelatin (Nycomed, Amersham) in PBS. The secondary goat anti-rabbit IgG antibody was coupled to 10 nm colloidal gold (British BioCell, UK). The antibody complex was stabilized with 1% glutaraldehyde in PBS and the labeled sections were poststained as described.

Acknowledgments

The authors thank Jana Müntler for excellent technical assistance and Arshad Desai for microscopy advice and many helpful discussions during the course of this work. For comments on the manuscript, we thank Arshad Desai and Eva Hannak. We are very grateful to: Yuji Kohara (National Institute of Genetics, Mishima, Japan) for cDNAs used in this study; Geraldine Seydoux (Johns Hopkins University, Baltimore, Maryland) and Judith Austin (University of Chicago, Chicago, Illinois) for vectors and advice on germline expression; Martin Srayko for *C. elegans* cDNA; and Sonja Rybina for help with antibody production. Karen Oegema was supported by a fellowship from the Helen Hay Whitney Foundation.

Received: August 22, 2002
Revised: February 4, 2003

References

Albertson, D.G. (1984). Formation of the first cleavage spindle in nematode embryos. Dev. Biol. *101*, 61–72.

Bobinnec, Y., Khodjakov, A., Mir, L.M., Rieder, C.L., Edde, B., and Bornens, M. (1998). Centriole disassembly in vivo and its effect on centrosome structure and function in vertebrate cells. J. Cell Biol. *143*, 1575–1589.

Bornens, M. (2002). Centrosome composition and microtubule anchoring mechanisms. Curr. Opin. Cell Biol. *14*, 25–34.

Callaini, G., and Riparbelli, M.G. (1990). Centriole and centrosome cycle in the early *Drosophila* embryo. J. Cell Sci. *97*, 539–543.

Cavalier-Smith, T. (2002). The phagotrophic origin of eukaryotes and phylogenetic classification of Protozoa. Int. J. Syst. Evol. Microbiol. *52*, 297–354.

Chapman, M.J., Dolan, M.F., and Margulis, L. (2000). Centrioles and kinetosomes: form, function and evolution. Q. Rev. Biol. *75*, 409–429.

Fry, A.M., Meraldi, P., and Nigg, E.A. (1998). A centrosomal function for the human Nek2 protein kinase, a member of the NIMA family of cell cycle regulators. EMBO J. *17*, 470–481.

Fry, A.M., Mayor, T., and Nigg, E.A. (2000). Regulating centrosomes by protein phosphorylation. Curr. Top. Dev. Biol. *49*, 291–312.

Gönczy, P., Echeverri, C., Oegema, K., Coulson, A., Jones, S.J., Copley, R.R., Duperon, J., Oegema, J., Brehm, M., Cassin, E., et al. (2000). Functional genomic analysis of cell division in *C. elegans* using RNAi of genes on chromosome III. Nature *408*, 331–336.

Gould, R.R., and Borisy, G.G. (1977). The pericentriolar material in Chinese hamster ovary cells nucleates microtubule formation. J. Cell Biol. *73*, 601–615.

Hamill, D.R., Severson, A.F., Carter, J.C., and Bowerman, B. (2002). Centrosome maturation and mitotic spindle assembly in *C. elegans* require SPD-5, a protein with multiple coiled-coil domains. Dev. Cell *3*, 673–684.

Hannak, E., Kirkham, M., Hyman, A.A., and Oegema, K. (2001). Aurora-A kinase is required for centrosome maturation in *Caenorhabditis elegans*. J. Cell Biol. *155*, 1109–1116.

Hannak, E., Oegema, K., Kirkham, M., Gonczy, P., Habermann, B., and Hyman, A.A. (2002). The kinetically dominant assembly pathway

for centrosomal asters in *Caenorhabditis elegans* is γ-tubulin dependent. J. Cell Biol. *157*, 591–602.

Kochanski, R.S., and Borisy, G.G. (1990). Mode of centriole duplication and distribution. J. Cell Biol. *110*, 1599–1605.

Kuriyama, R., and Borisy, G.G. (1981). Centriole cycle in Chinese hamster ovary cells as determined by whole-mount electron microscopy. J. Cell Biol. *91*, 814–821.

Lange, B.M., Faragher, A.J., March, P., and Gull, K. (2000). Centriole duplication and maturation in animal cells. Curr. Top. Dev. Biol. *49*, 235–249.

Lonsdale, J.E., McDonald, K.L., and Jones, R.L. (2001). Microwave polymerisation in thin layers of London Resin White allows selection of specimens for immunogold labelling. In Microwave Techniques and Protocols, T. Giberson and R.S. Demaree, eds. (Totowa, NJ: Humana Press), pp. 139–153.

Marshall, W.F. (2001). Centrioles take center stage. Curr. Biol. *11*, R487–496.

Matthews, L.R., Carter, P., Thierry-Mieg, D., and Kemphues, K. (1998). ZYG-9, a *Caenorhabditis elegans* protein required for microtubule organization and function, is a component of meiotic and mitotic spindle poles. J. Cell Biol. *141*, 1159–1168.

Mayor, T., Stierhof, Y.D., Tanaka, K., Fry, A.M., and Nigg, E.A. (2000). The centrosomal protein C-Nap1 is required for cell cycle-regulated centrosome cohesion. J. Cell Biol. *151*, 837–846.

Mazia, D., Harris, P.J., and Bibring, T. (1960). The multiplicity of the mitotic centers and the time-course of their duplication and separation. J. Biophys. Biochem.Cytol. *7*, 1–20.

Mignot, J.P. (1996). The centrosomal big bang: from a unique central organelle towards a constellation of MTOCs. Biol. Cell *86*, 81–91.

Montgomery, M.K., and Fire, A. (1998). Double-stranded RNA as a mediator in sequence-specific genetic silencing and co-suppression. Trends Genet. *14*, 255–258.

Moritz, M., Zheng, Y., Alberts, B.M., and Oegema, K. (1998). Recruitment of the γ-tubulin ring complex to *Drosophila* salt-stripped centrosome scaffolds. J. Cell Biol. *142*, 775–786.

O'Connell, K.F., Caron, C., Kopish, K.R., Hurd, D.D., Kemphues, K.J., Li, Y., and White, J.G. (2001). The *C. elegans* zyg-1 gene encodes a regulator of centrosome duplication with distinct maternal and paternal roles in the embryo. Cell *105*, 547–558.

Oakley, B.R. (2000). γ-Tubulin. Curr. Top. Dev. Biol. *49*, 27–54.

Oegema, K., Desai, A., Rybina, S., Kirkham, M., and Hyman, A.A. (2001). Functional analysis of kinetochore assembly in *Caenorhabditis elegans*. J. Cell Biol. *153*, 1209–1226.

Palazzo, R.E., Vogel, J.M., Schnackenberg, B.J., Hull, D.R., and Wu, X. (2000). Centrosome maturation. Curr. Top. Dev. Biol. *49*, 449–470.

Piel, M., Meyer, P., Khodjakov, A., Rieder, C.L., and Bornens, M. (2000). The respective contributions of the mother and daughter centrioles to centrosome activity and behavior in vertebrate cells. J. Cell Biol. *149*, 317–330.

Praitis, V., Casey, E., Collar, D., and Austin, J. (2001). Creation of low-copy integrated transgenic lines in *Caenorhabditis elegans*. Genetics *157*, 1217–1226.

Preble, A.M., Giddings, T.M., Jr., and Dutcher, S.K. (2000). Basal bodies and centrioles: their function and structure. Curr. Top. Dev. Biol. *49*, 207–233.

Priess, J.R., and Hirsh, D.I. (1986). *Caenorhabditis elegans* morphogenesis: the role of the cytoskeleton in elongation of the embryo. Dev. Biol. *117*, 156–173.

Rappleye, C.A., Paredez, A.R., Smith, C.W., McDonald, K.L., and Aroian, R.V. (1999). The coronin-like protein POD-1 is required for anterior-posterior axis formation and cellular architecture in the nematode *Caenorhabditis elegans*. Genes Dev. *13*, 2838–2851.

Rieder, C.L., and Borisy, G.G. (1982). The centrosome cycle in PtK2 cells: asymmetric distribution and structural changes in the pericentriolar material. Biol. Cell *44*, 117–132.

Rieder, C.L., Faruki, S., and Khodjakov, A. (2001). The centrosome in vertebrates: more than a microtubule-organizing center. Trends Cell Biol. *11*, 413–419.

Schnackenberg, B.J., Khodjakov, A., Rieder, C.L., and Palazzo, R.E. (1998). The disassembly and reassembly of functional centrosomes in vitro. Proc. Natl. Acad. Sci. USA *95*, 9295–9300.

Schumacher, J.M., Ashcroft, N., Donovan, P.J., and Golden, A. (1998). A highly conserved centrosomal kinase, AIR-1, is required for accurate cell cycle progression and segregation of developmental factors in *C. elegans* embryos. Development *125*, 4391–4402.

Sluder, G., and Rieder, C.L. (1985). Centriole number and the reproductive capacity of spindle poles. J. Cell Biol. *100*, 887–896.

Sluder, G., and Hinchcliffe, E.H. (1999). Control of centrosome reproduction: the right number at the right time. Biol. Cell *91*, 413–427.

Timmons, L., Court, D.L., and Fire, A. (2001). Ingestion of bacterially expressed dsRNAs can produce specific and potent genetic interference in *Caenorhabditis elegans*. Gene *263*, 103–112.

Vorobjev, I.A., and Chentsov, Y.S. (1982). Centrioles in the cell cycle. I. Epithelial cells. J. Cell Biol. *93*, 938–949.

Vorobjev, I.A., and Nadezhdina, E.S. (1987). The centrosome and its role in the organization of microtubules. Int. Rev. Cytol. *106*, 227–293.

Wolf, N., Hirsh, D., and McIntosh, J.R. (1978). Spermatogenesis in males of the free-living nematode, *Caenorhabditis elegans*. J. Ultrastruct. Res. *63*, 155–169.

Zipperlen, P., Fraser, A.G., Kamath, R.S., Martinez-Campos, M., and Ahringer, J. (2001). Roles for 147 embryonic lethal genes on *C. elegans* chromosome I identified by RNA interference and video microscopy. EMBO J. *20*, 3984–3992.